Journal Name

COMMUNICATION

Shaping Metal-Organic Framework Materials with A Honeycomb Internal Structure

Yingya Zhang,[a] Juanjuan Cai,[a] Dayou Zhang,[b] Xuebin Ke,*[c] and Lixiong Zhang*[a]

A self-assembly technology allows metal-organic framework materials to constitute a honeycomb internal structure while being shaped into millimeter-scale spheres. The ZIF-8 load is up to 83 wt% through solidification of chitosan (CS). This approach can be expanded to other morphologies (fibers) or crystals and is transformative for industrial manufacturing of nanomaterials.

Metal-organic frameworks (MOFs), as a class of ordered porous materials, are synthesized from metal ions and organic ligands.[1] MOFs are recognized to have potential applications in adsorption separation, heterogeneous catalysis, and gas storage, thus attracting great interest in both academic and industrial communities.[2-4] Shaping MOFs of fine particles into various geometries is becoming the crucial procedure for industrial use.

The shaping process for industrial zeolites (other porous materials) has been well established, which is to mix zeolite powders and inorganic binders, followed by moulding and calcination.[5] Unfortunately, MOFs cannot stand a high calcination temperature. To this end, electrospinning and crosslinking are used to blend MOF particles with polymers, such as polystyrene, polyvinyl pyrrolidone, polyacrylonitrile, and nanocellulose biopolymers.[6,7] Although a high load (50-80 wt%) of MOF particles can be achieved, several serious drawbacks impede the extensive application, such as non-uniform particle distributions, loose particle-polymer interaction, and pore blockages.[8] The internal phase emulsion is used to combine the crystallization of MOF precursors with the polymerization of monomers.[8-10] However, large amounts of surfactants are consumed and the content of MOFs is very limited (< 15 wt%).

An in-situ growth technique is developed to synthesize MOFs within the polymer matrix, where the binding of metal ions to polymer is crucial. Surface modification and atomic layer deposition are applied to facilitate the growth of MOFs within/on the substrate.[9,10] ZIF-8-, MIL-100(Fe)-, and ZIF-67-alginate beads, fibers and membranes are obtained by first crossing-linking alginate with M^{n+} (M=Cu, Zn, Fe, Co) to form engineering hydrogels, followed by post-treatment in MOF ligand solution.[11] Chitin-Cu_3BTC_2 fibers are prepared by incubating chitinous fibers in a $Cu(NO_3)_2$ solution, followed by reaction with trimesic acid.[12] The in-situ fabrication simplifies the procedure and processes the MOFs into various shapes. However, the MOF loads are very low (24-53 wt%). Moreover, the polymer networks have limited porosity for mass diffusion and the sufficient exchange of metal ions for crystal growth takes a long time (> 2 days).[11]
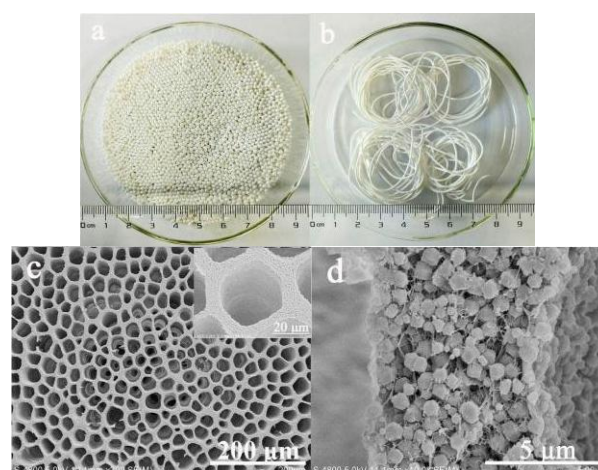

Fig. 1 Optical photographs and SEM images of typical ZIF-8/CS composites: (a) microspheres; (b) fibers; (c) channel structures; (d) the honeycomb wall between adjacent channels. The inset shows honeycomb channels.

a. State Key Laboratory of Materials-Oriented Chemical Engineering and College of Chemistry and Chemical Engineering, Nanjing Tech University, Nanjing 210009, PR China. E-mail: lixiongzhang@yahoo.com
b. College of Overseas Education, Nanjing Tech University, Nanjing 210009, PR China
c. School of Engineering and Computer Science, University of Hull, HU6 7RX, United Kingdom. E-mail: x.ke@hull.ac.uk

Recently, our group developed an impregnation-gelation-hydrothermal technique to prepare hybrid microspheres and hollow fibers consisting of zeolites and chitosan (CS).[13,14] The CS microspheres are immediately formed while adding a CS solution to a alkaline solution (**Figure S1**). The chitosan of a large molecular weight can only dissolve in acidic or neutral solution due to the protonization of -NH$_2$ groups. In alkaline conditions the solidification of CS can quickly happen along the outer surface of the droplets and subsequently transfer inwards. This fabrication stimulates a solution to shape MOF powders. In this work, the crystal growth is combined with the CS shaping in a single step. The obtained ZIF-8 crystals are well dispersed within CS matrix, yielding ZIF-8/CS microspheres. The ZIF-8/CS composites have a honeycomb internal structure and a high load of ZIF-8 crystals. The ordered porosity certaily has some enhanced properties in terms of mechanical and thermal stability.[15,16] We extend the technique to other morphologies (fibers) and other crystalline materials (ZIF-7 and ZIF-67), and showcase the adsorption capability to metal ions.

Synthesis of ZIF-8/CS composites. A simple self-assembly process can produce microspheres or fibers of a high yield. When we add the solution of Zn(NO$_3$)$_2$ and CS into a mixture solution of NaOH and 2-Methylimidazole (Hmim), the solidification occurs immediately and forms CS microspheres. Meanwhile, Zn^{2+} in the microspheres reacts with Hmim in the solution, resulting in the growth of ZIF-8 crystals. The spheres exhibit a size of 2 mm in diameter and the fibers have a diameter around 1 mm with a random length even up to 1 meter (**Figure 1**). The oriented micro-channels are assembled with a passage size about 25 μm (Figure 1c). From the cross-section, the thickness between the adjacent channels is 5 μm, composed of 500 nm sized particles of a rhombic dodecahedron morphology (Figure 1d). ZIF-8/CS microspheres with honeycomb internal structure are successfully prepared. The outer-wall of spheres is full of ZIF-8 crystals within CS matrix (**Figure S2**). The size of Zn^{2+}-CS aqueous droplets can be controlled by using different needles or microfluidic reactors and thus the size of microspheres/fibers is readily adjustable.

The XRD patterns confirm a high crystallinity of ZIF-8/CS microspheres and the FT-IR spectra reveal characteristic absorption bands assigned to chitosan and ZIF-8 crystals (**Figure S3**).[17] The broad band at 3482 cm^{-1}, corresponding to the stretching vibration of hydroxyl, amino and amide groups in chitosan, shifts to 3440 cm^{-1}, which indicates the formation of hydrogen bonds between -NH$_2$ radicals of ZIF-8 and chitosan. The bands at 1653 cm^{-1} and 1598 cm^{-1} assigned to amide groups in chitosan indicate strong interactions between amide groups and zinc ions. The sharp peak at 421 cm^{-1} related to Zn–N bond is ascribed to the introduction of ZIF-8 crystals.[17-20]

The ZIF-8 loads in the ZIF-8/CS microspheres can be estimated to be 68 wt% from TG analysis and Nitrogen adsorption-desorption isotherms show that the specific surface area is 1076 m^2 g^{-1} with a pore volume of 425.3 cm^3 g^{-1} (**Figure S4**). As the specific surface area of CS microspheres is only 7.4 m^2 g^{-1}, we can estimate the surface area of ZIF-8
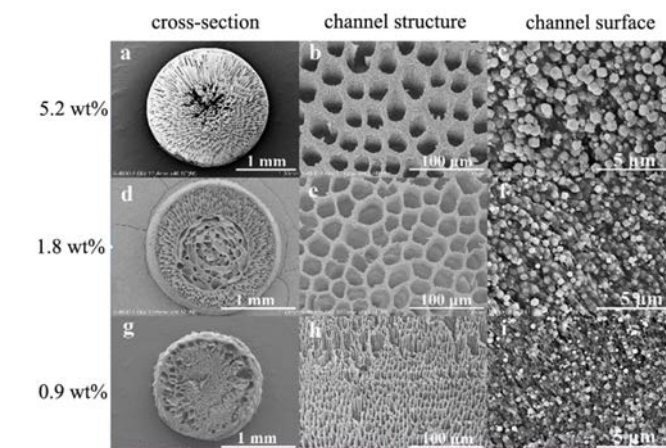

Fig. 2 SEM images of ZIF-8/CS hybrid microspheres prepared with different Zn(NO$_3$)$_2$ concentrations.

crystals is 1580 m^2 g^{-1}.[21] The CO$_2$ adsorption isotherm of the ZIF-8/CS microspheres indicates that the CO$_2$ adsorption amount is 0.57 mmol/g and equivalent to 0.84 mmol/g of pure ZIF-8 (**Figure S5**), which is comparable to the reported results.[22] The ZIF-8/CS composites reveal that we can assemble ZIF-8 nanocrystals into the shaped microspheres, without deteriorating the physical property of ZIF-8 crystals themselves.

The inner structure and ZIF-8 content in the hybrid microspheres can be adjusted by changing the Zn(NO$_3$)$_2$ amounts, without changing the molar ratio of Zn^{2+} to Hmim. When we decrease the Zn(NO$_3$)$_2$ content from 5.2 wt% to 0.9 wt%, ZIF-8/CS composite microspheres are obtained with regular porous structure (**Figure 2**). However, the inner structure evolves obviously, from a spherical shell to an internal hollow structure (Figure 2a), composed of regular honeycomb channels (Figure 2b). The formation of a hollow structure may be ascribed to the fast reaction of Zn^{2+} with Hmim around the outer surface of aqueous droplets and the drawing of Zn^{2+} from the center to the shell. The thickness between the adjacent channels is about 5 μm, composed of 500 nm sized particles (Figure 2c). When we lower the Zn(NO$_3$)$_2$ content down to 0.9 wt%, the XRD patterns confirm the formation of ZIF-8 crystals and the N$_2$ absorption-desorption isotherms show that their specific surface areas are 1309 m^2/g (for 1.8 wt%) and 469 m^2/g (for 0.9 wt%), respectively (**Figure S6**).For the low Zn(NO$_3$)$_2$ content, uniform ZIF-8 crystals are shown on the surface (Figure 2f and 2i). The channel size becomes smaller down to 10 μm (Figure 2h) as well as the size (200 nm) of ZIF-8 particles (Figure 2i). However, the channel size is not linear with the Zn(NO$_3$)$_2$ content and many factors influence on the assembly of the honeycomb channels, such as the thickness of channel walls and the diffusion of active components inside microspheres. Furthermore, decreasing Zn(NO$_3$)$_2$ content to 0.45 wt%, irregular microspheres and pores (**Figure S7**) are obtained. The TG curves of these microspheres determine that the ZIF-8 loads range between 83 wt% and 30 wt%, mainly depending on the Zn(NO$_3$)$_2$ content (**Figure S8**).

The morphologies of the ZIF-8/CS composites are adjustable by using different techniques. Herein, we demonstrate the preparation of ZIF-8/CS hybrid fibers by a microfluidic spinning method (Figure S1). The obtained hybrid fibers have a random length and controllable size (Figure 1d). More importantly, a core/shell structure is formed with a porous and axial-oriented channel, slightly different from the inner structure of the microspheres (**Figure S9**).

To explore the function of Zn^{2+} in the formation of the honeycomb structure, we observe the inner structure evolution of CS using the same procedure but without Zn^{2+} addition. No uniform porous structures are formed in CS microspheres alone, while honeycomb porous networks present in Zn^{2+}/CS microspheres with $Zn(NO_3)_2$ content of 1.8 wt% or below (**Figure S10**). These results indicate that small amounts of Zn^{2+} are necessary and the interaction between Zn^{2+} and CS contributes to assemble a honeycomb porous structure. CS can be protonated by acetic acid and adsorb Zn^{2+} by ion-exchange to form the metal-chitosan complex.[23] Such complex can be solidified to form microspheres in alkaline conditions. During this process, rearrangement of chitosan occurs to form a cellular porous structure (Figure S10). Such structure becomes uniform and stable after freeze-drying, possibly ascribed to the ice-template mechanism.[24] Therefore, the interaction between Zn^{2+} and chitosan, assembly of Zn^{2+}-chitosan complex, and freeze-drying all contribute to the formation of a stable cellular porous structure. The subsequent reaction of Zn^{2+} with Hmim does not have significant influence on the porous structure.

Synthesis of ZIF-7/CS and ZIF-67/CS composites. The proposed mechanism suggests that the ion-chitosan interaction enables the cellular porous structures during the CS solidification. We then examine the interaction between various metal ions and chitosan. Among them, Ca^{2+}, Fe^{3+}, Ni^{2+}, Co^{2+} and Zn^{2+} are applicable to form the cellular porous structures (**Figure S11**). We then take ZIF-7 and ZIF-67 as examples to prepare MOF/CS microspheres, as the former uses Zn^{2+} as the sources of metal ions and the latter uses Co^{2+}.

Following the same procedure we first prepare ZIF-7/CS microspheres using the ligand of benzimidazol. Similarly, the honeycomb internal structure is observed with porous passages, and the microchannels have pore size about 25 μm (**Figure 3**). The XRD pattern confirms that ZIF-7 crystals are produced within CS microspheres (**Figure S12**). The thickness
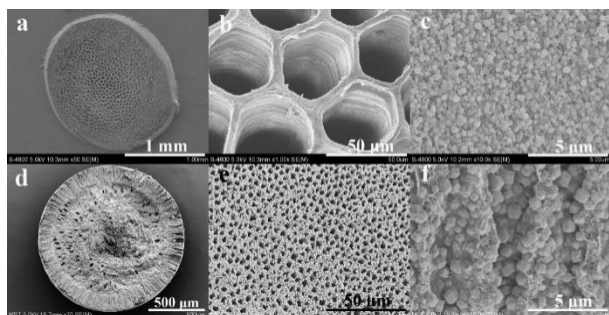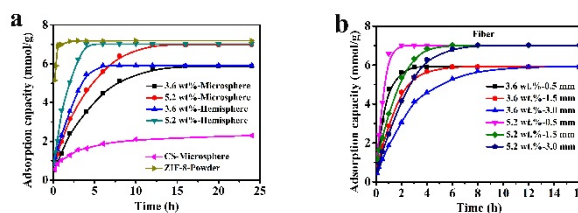

Fig. 4 The adsorption curves of Cu(II) for ZIF-8/CS microspheres (a) and fibers (b).

between the adjacent channels is 2 μm, composed of 200 nm sized ZIF-7 nanoparticles (**Figure S13**). We also prepared ZIF-67/CS microspheres, which contains Co^{2+} as the metal ion source. XRD patterns verify the successful synthesis of these MOFs (**Figure S14**) and SEM images show their inner structure (Figure 3). The shell is composed of oriental microchannels with the channel size of 4 μm (**Figure S15**).

Adsorption performance of ZIF-8/CS composites. These composites are soft and compressible and can float on water surface, which are excellent materials for pollutants removal. We apply the ZIF-8/CS composites in the adsorption of Cu(II) in water.[25,26] The results indicate that the composites have an equilibrium adsorption amount for Cu(II) of 5.9 mmol/g and 7.0 mmol/g when the $Zn(NO_3)_2$ content is 3.6 wt% and 5.2 wt%, respectively, whatever in a shaped geometry of spheres or fibers (**Figure 4**). As the cross-linked CS aerogels show an adsorption capacity of 2.3 mmol/g for Cu(II) ions, the corresponding adsorption capacity of pure ZIF-8 is 7.2 mmol/g.

The paramount advantage of ZIF-8/CS composites is the rate to reach a constant adsorption amount, depending on the ZIF-8 loads and the geometry. The fibers take shorter time than the microspheres with comparable sizes. This can be attributed to the open structure of the fibers, compared with more dense shell of the microspheres. To verify this, we cut the microspheres into hemispheres so that the inner honeycomb structure is exposed. The time to reach adsorption equilibrium for the hemispheres is only 2/3 of that for the microspheres. For the hybrid fibers the adsorption differs significantly when their length changes from 0.5 mm to 3 mm, due to the long diffusion path. These results demonstrate that moulding of MOFs does not have any damage to the MOFs properties. Further results show that it takes 1 hour (for fibers) and 10 hours (for microspheres) to adsorb 85 wt% of Cu(II), respectively. Similarly it takes 24 hours for the UiO-66/nanocellulose aerogels to adsorb the same amount of metal ions.[6,7] The ZIF-8/CS composites exhibit a fast diffusion rate which can be ascribed to their porous internal structures.

We have demonstrated a facile method to incorporate ZIF-8 particles into CS substrates to form ZIF-8/CS microspheres/fibers. ZIF-8 particles are well dispersed and embedded into the CS matrix. The ZIF-8 loads can be up to 83 wt% and tailored by changing initial concentrations of $Zn(NO_3)_2$. The ZIF-8/CS microspheres show a specific surface area of 1309 m^2/g and a regular honeycomb structure. Other two of MOF/CS composites are obtained using different metal ions or ligand molecules, such as ZIF-7 and ZIF-67, highlighting

Fig. 3 SEM images of the inner structures of the ZIF-7/CS (a-c) and ZIF-67/CS (d-f) microspheres.

the versatility of this method. The mechanistic study reveals that the rearrangement of CS occurs to form cellular porous structure during solidification. The Zn^{2+}-chitosan composites could be in situ converted into ZIF-8/CS composites. The ZIF-8/CS composites are effective absorbents to remove Cu(II), showing a high adsorption capacity and a large adsorption rate. This simple method can incorporate crystalline particles into CS matrix and the honeycomb internal structure will facilitate the shaped materials for direct industrial use.

Conflicts of interest

There are no conflicts to declare.

Notes and references

1 H. Li, M. Eddaoudi, M. O'Keeffe and O. M. Yaghi, *Nature* 1999, **402**, 276-279.
2 F. Luo, C. Yan, L. Dang, R. Krishna, W. Zhou, H. Wu, X. Dong, Y. Han, T. L. Hu, M. O'Keeffe, L. Wang, M. Luo, R. B. Lin and B. Chen, *J. Am. Chem. Soc.* 2016, **138**, 5678-5684.
3 U. P. N. Tran, K. K. A. Le and N. T. S. Phan, *ACS Catal.* 2011, **1**, 120-127.
4 D. Alezi, Y. Belmabkhout, M. Suyetin, P. M. Bhatt, L. J. Weselinski, V. Solvyeva, K. Adil, I. Spanopoulos, P. N. Trikalitis, A. Emwas and M.Eddaoudi, *J. Am. Chem. Soc.* 2015, **137**, 13308-13318.
5 N. L. Michels, S. Mitchell and J. Pérezramírez, *ACS Catal.* 2014, **4**, 2409-2417.
6 R. Ostermann, J. Cravillon, C. Weidmann, M. Wiebcke and B. M. Smarsly, *Chem. Commun.* 2010, **47**, 442-444.
7 H. Zhu, X. Yang, E. D. Cranston and S. Zhu, *Adv. Mater.* 2016, **28**, 7652-7657.
8 S. Li and F. Huo, *Nanoscale.* 2015, **7**, 7482-7501.
9 M. Meilikhov, K. Yusenko, E. Schollmeyer, C. Mayer, H. Buschmann and R. A. Fischer, *Dalton T.* 2011, **40**, 4838-4841.
10 J. Zhao, M. D. Losego, P. C. Lemaire, P. S. Williams, B. Gong, S. E. Atanasov, T. M. Blevins, C. J. Oldham, H. J. Walls, S. D. Shepherd, M. A. Browe, G. W. Peterson and G. N. Parsons, *Adv. Mater. Interfaces.* 2014, **1**, 1400040.
11 H. Zhu, Q. Zhang and S. Zhu, *ACS Appl. Mater. Inter.* 2016, **8**, 17395-17401.
12 D. Wisser, F. M. Wisser, S. Raschke, N. Klein, M. Leistner, J. Grothe and E. Brunner, *Angew. Chem.Int. Ed.* 2015, **54**, 12588-12591.
13 L. Yu, J. Gong, C. Zeng and L. Zhang, *Ind. Eng. Chem. Res.* 2012, **51**, 2299-2308.
14 L. Yu, C. Zeng, C. Wang and L. Zhang, *Microporous Mesoporous Mater.* 2016, **244**, 278-283.
15 X. Xu, L. Heng, X. Zhao, J. Ma, L. Lin and L. Jiang, *J. Mater. Chem.* 2012, **22**, 10883-10888.
16 L. Heng, J. Li, M. Li, D. Tian, L. Fan, L. Jiang and B.Z.Tang, *Adv. Funct. Mater.* 2014, **24**, 7241-7248.
17 K. S. Park, Z. Ni, A. P. Cote, J. Y. Choi, R. Huang, F. J. Uribe-Romo, H. K. Chae, M. O'Keeffe and O. M. Yaghi, *Proc. Nat. Acad. Sci. USA.* 2006, **103**, 10186-10191.
18 Y. Hu, H. Kazemian, S. Rohani, Y. Huang and Y. Song, *Chem. Commun.* 2011, **47**, 12694-12696.
19 X. Gao, H. Xiao, H. Baigude, W. Guan and Z. Liu, *Sci. Rep.* 2016, **6**, 37705.
20 Y. Han, P. Qi, S. Li, X. Feng, J. Zhou, H. Li, S. Su, X. Li and B. Wang, *Chem. Commun.* 2014, **50**, 8057-8060.
21 A. Moosa, A. M. Ridha and A. Kadim, *Am. J. Mater. Sci.* 2016, **6**, 95-104.
22 G. Kontos, V. Likodimos, C. M. Veziri, E. Kouvelos, N. Moustakas, G. N. Karanikolos and G. E. Romanos, *Chemsuschem.* 2014, **7**, 1696-1702.
23 X. Liu, Q. Hu, Z. Fang, X. Zhang and B. Zhang, *Langmuir* 2009, **25**, 3-8.
24 M. C. Gutiérrez, M. L. Ferrer and F. D. Monte, *Chem. Mater.* 2008, **20**, 634-648.
25 A. Li, R. Lin, C. Lin, B. He, T. Zheng, L. Lu and Y. Cao, *Carbohydr. Polym.* 2016, **148**, 272-280.
26 Y. Zhao, Y. Pan, W. Liu and L. Zhang, *Chem. Lett.* 2015, **44**, 758-760.